Journal of Magnetism and Magnetic Materials 345 (2013) 153–158

Contents lists available at SciVerse ScienceDirect

Journal of Magnetism and Magnetic Materials

journal homepage: www.elsevier.com/locate/jmmm

Magnetocaloric effect and refrigerant capacity in melt-spun Gd–Mn alloys

Tanjore V. Jayaraman [a,b,*], Laura Boone [a], Jeffrey E. Shield [a,b]

[a] Department of Mechanical and Materials Engineering, University of Nebraska, Lincoln 68588, US
[b] Nebraska Center for Materials and Nanoscience, University of Nebraska, Lincoln 68588, US

ARTICLE INFO

Article history:
Received 14 March 2013
Received in revised form
5 June 2013
Available online 26 June 2013

Keywords:
Magnetocaloric
Refrigerant capacity
Gd–Mn alloy
Melt-spun

ABSTRACT

The magnetocaloric properties and microstructure of melt-spun $Gd_{100-x}Mn_x$ ($x=0$, 5, 10, 15, and 20 at%) alloys were investigated to explore their potential application as room-temperature magnetic refrigerants. The alloys were composed of nanostructured hexagonal α-Gd phase with grain sizes between 40 and 150 nm. Increasing the Mn content resulted in a decrease in the lattice parameters (a and c) of Gd, suggesting the formation of a substitutional solid solution. The Curie temperature (T_C), derived from M–T curves and Arrot plots, decreased monotonically from ~293 K (melt-spun Gd) to ~278 K (melt-spun $Gd_{80}Mn_{20}$). The saturation magnetization at 260 K decreased from ~108 emu/g (melt-spun Gd) to ~78 emu/g (melt-spun $Gd_{80}Mn_{20}$). The peak value of magnetic entropy change, $(-\Delta S_M)_{max}$, decreased from ~8.6 J/kgK for melt-spun Gd to ~5.9 J/kgK for melt-spun $Gd_{80}Mn_{20}$ alloy and the refrigeration capacity (RC) initially increased from ~433 J/kg for melt-spun Gd to ~452 J/kg for melt-spun $Gd_{95}Mn_5$ and then gradually decreased to ~321 J/kg for melt-spun $Gd_{80}Mn_{20}$, for a magnetic field varying from 0 to 5 T. The near-room temperature magnetocaloric properties of melt-spun $Gd_{100-x}Mn_x$ ($0 \le x \le 20$) alloys were found to be comparable to other magnetic refrigerants based on first-order phase transitions.

1. Introduction

There has been a profound interest in the research and development of magnetocaloric materials owing to their potential application in magnetic refrigeration or magnetic cooling. The magnetocaloric effect (MCE) was originally discovered in Fe by Warburg in 1881 [1]. Magnetic refrigeration near room temperature is of particular interest as it is an excellent alternative to vapor-compression refrigeration technology. It not only has the potential to reduce global energy consumption but also eliminate the use of ozone depleting compounds (chlorofluorocarbons), greenhouse gases (hydrochlorofluorocarbons and hydrofluorocarbons), and hazardous chemicals (ammonia) [2–8]. The MCE is represented by adiabatic temperature change (ΔT_{ad}) or isothermal magnetic entropy change (ΔS_M), which is a function of both temperature (T) and magnetic field change (ΔH). The MCE (ΔS_M and ΔT_{ad}) may be either measured directly or calculated indirectly from the experimentally measured magnetization and/or heat capacity [4,5,8]. Along with ΔS_M, the refrigerant capacity (RC) is also an accepted criterion to evaluate refrigeration efficiency [4]. Hence to obtain a large RC a broad ΔS_M–T curve is also needed along with large ΔS_M.

Large MCEs (from cryogenic temperatures to room temperatures) have been observed in two kinds of magnetic materials: (a) materials that exhibit a first-order transition (FOT) undergo a simultaneous structural and magnetic phase transition that leads to a giant magnetic entropy change across its ordering temperature, accompanied by narrow working temperature range and large thermal and magnetic hysteresis losses (e.g., GdSiGe, MnAsSb, and LaFeSi alloys) [3,7,9,10]; and (b) materials that exhibit a second-order transition (SOT) undergo only a magnetic phase transition that leads to magnetic entropy change across its ordering temperature accompanied with negligible magnetic hysteresis, no thermal hysteresis, and over a comparatively broader temperature range (e.g., some rare earth metals, rare earth intermetallic alloys and some perovskites) [4,8].

The rare earth metal Gd is a popular SOT-based, near-room temperature magnetic refrigerant [2,4,5,8]. The cooling efficiency in magnetic refrigerators working with Gd is shown to reach 60% of the theoretical limit compared to only about 40% in the best vapor compression refrigerators [11,12]. The MCE for Gd peaks at the Curie temperature (T_C). Few of the current research efforts are towards developing suitable Gd based SOT magnetic refrigerants that display large MCE near room temperature in magnetic fields ~2 T or less so that such fields can be generated by permanent magnets or electromagnets [13–15]. In the past many binary Gd based alloys have been studied. Alloying of Gd with R (R=rare earth elements such as Tb, Ho, Dy, and Yb) decreases T_C and $(-\Delta S_M)_{max}$ [4,8]. Transition metal

* Corresponding author.
E-mail address: tvjayaraman@gmail.com (T.V. Jayaraman).

0304-8853/$ - see front matter © 2013 Elsevier B.V. All rights reserved.
http://dx.doi.org/10.1016/j.jmmm.2013.06.016

(T) additions have a variety of affects. T_C decreased when T=Ag, Co, Mn, V, Y, and Zn. $(-\Delta S_M)_{max}$ decreases for rapidly solidified Gd–Ag alloys and conventionally melted Gd–Zn alloys; remains constant for melt-spun Gd–Co alloys and as-cast Gd–Mn and Gd–Y alloys; and increases for as-cast Gd–V alloys. Gd–Y and Gd–V alloys have higher refrigeration capacity and relative cooling power as compared to Gd [15–20]. Hydrogen-doped Gd (GdH_x) shows enhancement in both T_C and $(-\Delta S_M)_{max}$ [21]. Studies in Gd–X (X=B, C) alloys show a decrease in $(-\Delta S_M)_{max}$ upon alloying Gd [22–25].

The magnetocaloric effect of melt-spun Gd–Mn alloys has not been studied. In this work the magnetocaloric properties of melt-spun $Gd_{100-x}Mn_x$ (x=0, 5, 10, 15, and 20 at%) alloys were examined near room temperature (250–320 K) to explore their potential application as magnetic refrigerants near room temperature.

2. Materials and methods

Ingots of $Gd_{100-x}Mn_x$ (x=0, 5, 10, 15, and 20 at%) alloys were prepared from high purity (> 99.95 wt%) elemental constituents by arc-melting. The melting of the alloys was performed in an ultra-high-purity argon atmosphere. The arc-melted ingots were rapidly solidified by melt spinning at a tangential wheel velocity of 40 m/s. The melt spinning was performed under a high-purity argon environment at a chamber pressure of 0.5 atm. The melt-spun ribbons were analyzed by a Rigaku MultiFlex x-ray diffractometer with θ–θ geometry using Cu Kα radiation. Transmission electron microscopy (TEM) was performed using JEOL 2010 operating at 200 kV on ribbons thinned by ion milling with a Gatan Precision Ion Polishing system at 4.5 kV. The magnetic characterization was performed using a Quantum Design Magnetic Property Measurement System (MPMS-XL) in fields up to 5 T over a temperature range of 100–320 K. The accuracy of temperature measurement was $\pm$0.2 K and that for magnetization measurements was within $\pm$1%.

3. Results and discussion

Fig. 1(a) shows the x-ray diffraction spectra for melt-spun &QJ; $Gd_{100-x}Mn_x$ (x=0, 5, 10, 15, and 20 at%) alloys. The x-ray spectrum of as-cast $Gd_{80}Mn_{20}$ is shown as a representative of as-cast alloys for comparison. From the x-ray spectra the presence of hcp α-Gd phase in melt-spun Gd–Mn alloys can be determined. The binary Gd–Mn phase diagram predicts the presence of $GdMn_2$ along with hcp α-Gd upon equilibrium cooling for compositions $0 < x \leq 20$ [26]. The as-cast $Gd_{100-x}Mn_x$ (x=5, 10, 15, and 20 at%) alloys were shown to have $GdMn_2$ along with the hcp α-Gd phase [20]. The presence of $GdMn_2$ phase in the as-cast alloy can be inferred from the (311) peak of $GdMn_2$ at 2θ~38.5°. The other prominent peaks of $GdMn_2$, viz. (220) at 2θ~32.5° and (330) at 2θ~62°, coincide with the peaks of α-Gd phase, viz. (101) at 2θ~32.5° and (201) at 2θ~62° respectively. However in the x-ray spectra for the melt-spun alloys the reflections corresponding to $GdMn_2$ were not observed. This suggests that the rapid solidification has suppressed the formation of $GdMn_2$ in the melt-spun $Gd_{100-x}Mn_x$ ($0 < x \leq 20$) alloys. In the melt-spun alloys, the (002) reflections were

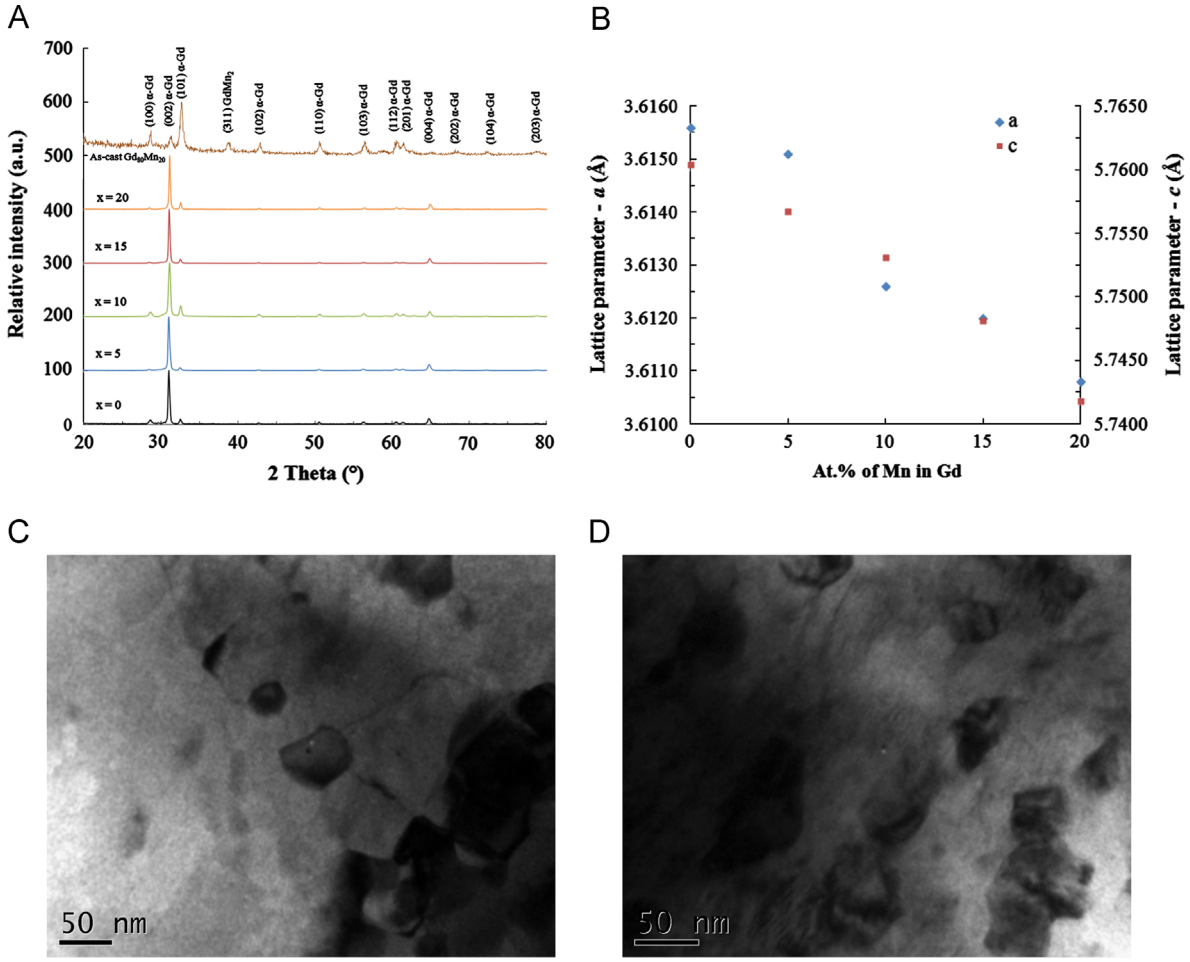

Fig. 1. (A) X-ray diffraction spectra of melt-spun $Gd_{100-x}Mn_x$ (x=0, 5, 10, 15, and 20) alloys and as-cast $Gd_{80}Mn_{20}$ alloy, (B) Variation of lattice parameters (a and c) in melt-spun $Gd_{100-x}Mn_x$ (x=0, 5, 10, 15, and 20) alloys, and Transmission electron micrographs of melt-spun (C) $Gd_{95}Mn_5$ and (D) $Gd_{85}Mn_{15}$ alloy.